

## Development and Validation of Partial Pressure of Carbon Dioxide Algorithm in the Southwest Bay of Bengal

R. Shanthi<sup>1</sup>, D. Poornima<sup>1</sup>, T. Thangaradjou<sup>1,\*</sup>, A. Saravanakumar<sup>1</sup>, S.B. Choudhry<sup>2</sup>

<sup>1</sup>Centre of Advanced Study in Marine Biology, Faculty of Marine Sciences, Annamalai University, Parangipettai 608502, Tamilnadu, India.

<sup>2</sup>National Remote sensing Centre, Balanagar, Hyderabad-500 625, Andhra Pradesh, India.

### Abstract

The primary productivity in the upper ocean is also a key factor associated with the surface CO<sub>2</sub>. Therefore, there is a potential to remotely sense the surface *p*CO<sub>2</sub> using satellite data based on its correlation with SST and chlorophyll *a*. Hence, the *in-situ* SST and chlorophyll datasets have been regressed with the calculated *p*CO<sub>2</sub> three dimensionally for four different functions such as plane, paraboloid, Gaussian and Lorentzian. Among four functions parabolic function found to be better fit than other functions for postmonsoon with a R<sup>2</sup> of 0.783 and minimum standard error estimate (SEE) of ± 24.052 µatm. Thus, the postmonsoon parabolic algorithm was used to generate the *p*CO<sub>2</sub> image. The validation of MODIS-Aqua derived SST and chlorophyll based *p*CO<sub>2</sub> map showed better agreement with calculated *p*CO<sub>2</sub> with R<sup>2</sup> of 0.755 and SEE of ± 23.609 µatm. The better regression between *p*CO<sub>2</sub>, SST and chlorophyll suggest that the effects of biological activities on the spatial and temporal changes in *p*CO<sub>2</sub> of the southwest Bay of Bengal cannot be ignored. However, the RMSE (± 27.156 µatm) of present *p*CO<sub>2</sub> algorithm is appreciably high due to inbound errors in MODIS derived SST and chlorophyll data products. Hence, improvement in sensor technology and retrieval algorithm would definitely improve the retrieval of input parameters (SST and Chlorophyll *a*) which in turn useful in estimating *p*CO<sub>2</sub> and air-sea CO<sub>2</sub> flux precisely in the Bay of Bengal at large spatial and temporal scales.

**Keywords:** SST, chlorophyll, *p*CO<sub>2</sub>, regression, RMSE, SEE, paraboloid

---

\* Corresponding author: T. Thangaradjou  
E-mail address: umaradjou@gmail.com

## 1. INTRODUCTION

In the recent years, researchers are more and more interested in understanding the global carbon cycle in the changing global climate. As one of the most important reservoir of the earth's carbon, oceans play a vital role in regulating global atmospheric CO<sub>2</sub> concentration. By using accurate estimates of global sea surface partial pressure of CO<sub>2</sub> ( $p\text{CO}_2$ ), the ratio of net CO<sub>2</sub> uptake of global ocean can be measured, which can provide a support for further research of global carbon cycle<sup>1</sup>. The Indian Ocean has been shown to be a net sink of atmospheric CO<sub>2</sub>, although the north Indian Ocean is richer in CO<sub>2</sub> than the atmosphere<sup>2</sup>. Studies from the north Indian Ocean indicated that the Arabian Sea is a perennial source of atmospheric CO<sub>2</sub><sup>3,4,5</sup>, while the Bay of Bengal act as a seasonal sink<sup>6</sup>. Due to strong upwelling during the southwest monsoon, surface waters of the coastal region in the Arabian Sea show a substantial increase in dissolved inorganic carbon (DIC) accompanied by very high  $p\text{CO}_2$ <sup>7</sup>.

Generally, the solubility of CO<sub>2</sub> in seawater is temperature dependent; hence the variation in the  $p\text{CO}_2$  is mainly driven by thermodynamics. In a parcel of seawater with constant chemical composition,  $p\text{CO}_2$  would increase by 4% when the water is warmed about 1°C<sup>8,9</sup>. Bay of Bengal is much warmer than the Arabian Sea and is consistent with Levitus climatology<sup>10</sup> indicating a possibility of stronger stratification in the Bay of Bengal which make it as sink of atmospheric CO<sub>2</sub>. The exchange of CO<sub>2</sub> directly with the atmosphere at the mixed-layer waters is affected primarily by temperature (SST), dissolved inorganic carbon (DIC) levels and total alkalinity (TA), where SST is influenced by physical processes like mixing of water masses, DIC and TA are influenced by the biological processes (photosynthesis and respiration)<sup>11</sup>. The DIC in the surface ocean varies from an average value of 2150  $\mu\text{mol kg}^{-1}$  in Polar Regions to 1850  $\mu\text{mol kg}^{-1}$  in the tropics as a result of biological processes and reduce  $p\text{CO}_2$  by 4%<sup>12</sup>. Therefore, the effect of biological drawdown and temperature on surface water  $p\text{CO}_2$  is similar but the two effects are often compensating. Hence, the spatial and temporal distribution of  $p\text{CO}_2$  in surface waters and CO<sub>2</sub> flux is largely governed by a balance between the changes in seawater temperature, net biological utilization of CO<sub>2</sub> and the upwelling flux of CO<sub>2</sub> rich waters.

Satellite observations are more useful in distinguishing spatial-temporal variations of geophysical parameters over the global oceans from intra-seasonal to inter-annual time scales. In addition to the change of atmospheric CO<sub>2</sub> accumulation,  $p\text{CO}_2$  is also essential to study the changes in ocean biogeochemistry. As the temperature and upwelling process can well be recorded in SST and the biological utilization can be derived in terms of chlorophyll *a* concentration. Both these parameters are effectively been recorded from space which can result in retrieval of  $p\text{CO}_2$  through empirical algorithms. Various algorithms have been derived for different areas at varied spatial scales. Initially, Stephens et al.<sup>8</sup> produced the statistical relationship between  $p\text{CO}_2$

and SST in the north Pacific and concluded that the relation is sufficient to estimate  $p\text{CO}_2$  using satellite SST over the oligotrophic waters but not over the eutrophic waters with significant primary production. Likewise, many algorithms that relate SST to  $p\text{CO}_2$  followed, in the Arabian Sea<sup>13</sup>, in the Sargasso Sea<sup>14</sup>, in the equatorial Pacific<sup>15</sup>, in the north Pacific<sup>16,17</sup>, in the Bay of Biscay<sup>18</sup> and in the northern south China Sea<sup>8</sup>, but their applicability is limited by geographical region, season and time scale based on the data used to develop the relationship between variables.

Later, the inclusion of chlorophyll *a* along with SST was done in North Pacific<sup>16</sup> and South China Sea<sup>8</sup>. Sarma et al.<sup>17</sup> further developed a remote-sensing algorithm for  $p\text{CO}_2$ , by including SST, chlorophyll *a* and climatological salinity. Lohrenz and Cai<sup>19</sup> added chromophoric dissolved organic matter (CDOM) to derive sea surface salinity as a parameter in their remote-sensing algorithm for  $p\text{CO}_2$ . Recently, Zui et al.<sup>20</sup> and Qin et al.<sup>1</sup> proposed a regression equation for  $p\text{CO}_2$  with SST and chlorophyll *a* with a RMSE of 13.45  $\mu\text{atm}$  and 21.46  $\mu\text{atm}$  with the satellite derived  $p\text{CO}_2$  respectively. Similar such studies that relate SST and chlorophyll with  $p\text{CO}_2$  through empirical relation are scanty in the Bay of Bengal. Hence, the present study is attempted to develop a regional  $p\text{CO}_2$  algorithm using the relationships between *in-situ* SST, chlorophyll and calculated  $p\text{CO}_2$  and the best fit algorithm has been validated with the calculated  $p\text{CO}_2$  measurements for remote sensing applications.

## 2. MATERIALS AND METHODS

The present study was carried out along the Tamilnadu coast falling along the southwest Bay of Bengal region. Four sampling station covering the longitude and latitude viz. Chennai (80°23.9E-13°07.9N), Cuddalore (79°48.5E – 11°42.4N), Parangipettai (79°51.7E – 11°30.6N) and Karaikal (79°55.5E – 10°54.8N) (Fig.1) were fixed and regular monthly samplings were made from January 2013 to March 2017. The entire study period was classified into four seasons namely postmonsoon (January to March), summer (April to June) and premonsoon (south west monsoon - July to September) and monsoon (October –December) classified based on northeast monsoon prevails in the region. Northeast monsoon is an actual monsoon in the southwest Bay of Bengal which brings more rainfall over Tamilnadu coast with northeast monsoon winds. Whereas, during southwest monsoon, the strong southwesterly winds play vital role in the surface waters resulting the turbulence at surface and wind driven vertical mixing of water column but rainfall was very minimum in the southwest Bay of Bengal.

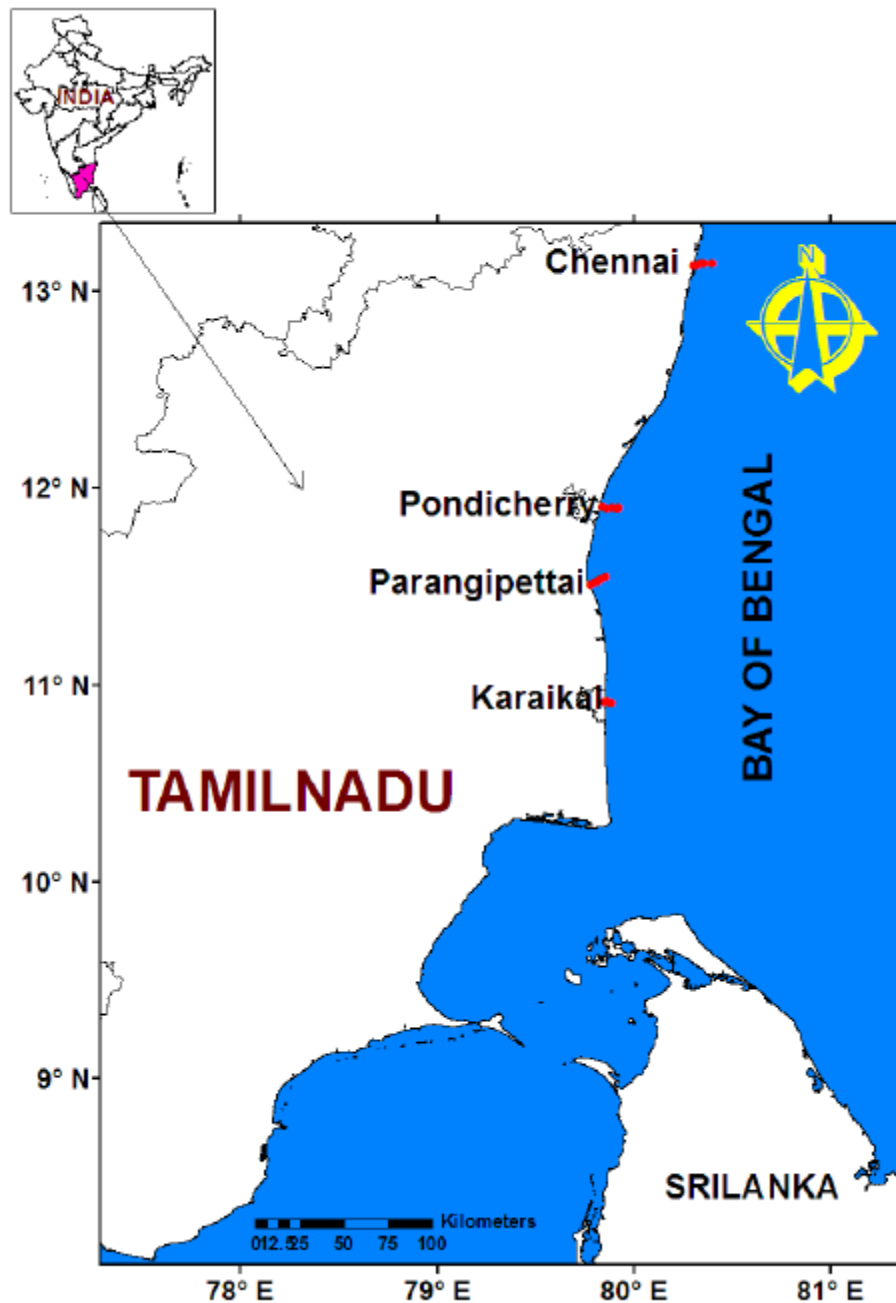


**Fig. 1.** Map showing the study area

### ***In-situ data***

*In-situ* SST was measured using digital multi-stem thermometer of 0.1° C accuracy. Water samples were collected using 5-litre Niskin water sampler and stored in polypropylene bottles (Tarson) in dark ice box and transported to laboratory. Chlorophyll *a* concentration was measured by following the method described by INCOIS<sup>21</sup> using spectrophotometer (Shimadzu- UV 2450) and it was calibrated with

standard chlorophyll *a* (Sigma C6144) using 90% acetone within 24 hours.

Salinity was measured using a hand held refractometer (Atago hand refractometer, Japan) and the pH was measured using a pH meter (EUTECH - cyberscan pH meter) with the accuracy of  $\pm 1\%$  and  $\pm 0.002$  respectively. Total alkalinity (TA) was measured using an automated titrator (905 potentiometric Titrando, Metrohm, Switzerland) by following the Gran titration method<sup>22</sup>. 0.1N stock solution of HCl was standardized by preparing standard solution of known alkalinity with analytical grade  $\text{Na}_2\text{CO}_3$ . DIC and  $p\text{CO}_2$  were computed based on measured SST, salinity, pH and TA using  $\text{CO}_2\text{CALC}$  program<sup>23</sup> by using the  $\text{CO}_2$  dissociation constants ( $k_1$  and  $k_2$ ) given by Lueker et al.<sup>24</sup>.

### SST and chlorophyll *a* based $p\text{CO}_2$ retrieval algorithm

*In-situ* SST, chlorophyll *a* and calculated  $p\text{CO}_2$  concentrations (595 data points) were obtained by monthly coastal samplings carried out at four sampling stations from January 2013 to March 2017 in the southwest Bay of Bengal region. The data points (15) matching with the date of satellite derived chlorophyll and SST data were treated separately for validation purposes. Finally, 580 points were taken for regression analysis accounting for  $\sim 97\%$  of the total data.

The primary productivity in the upper ocean is also a key factor associated with the surface  $\text{CO}_2$ . Therefore, there is a potential to remotely sense the surface  $p\text{CO}_2$  using satellite data based on its correlation with SST and chlorophyll *a*. Hence, the *in-situ* SST and chlorophyll datasets have been regressed with the  $p\text{CO}_2$  three dimensionally for four different functions such as plane, paraboloid, Gaussian, and Lorentzian (Table 1).

**Table 1.** Results of regression analysis between *in-situ* SST, chlorophyll and calculated  $p\text{CO}_2$

	N	Plane		Paraboloid		Gaussian		Lorentzian	
		R <sup>2</sup>	SEE(±)	R <sup>2</sup>	SEE(±)	R <sup>2</sup>	SEE(±)	R <sup>2</sup>	SEE (±)
Entire	580	0.804	76.174	0.809	75.266	0.815	74.104	0.811	74.811
Postmonsoon	165	0.778	24.154	<b>0.783</b>	<b>24.052</b>	0.637	31.090	0.632	31.298
Summer	120	0.690	42.870	0.700	42.370	0.535	52.781	0.522	53.486
Premonsoon	150	0.725	48.102	0.749	46.224	0.746	45.517	0.751	46.071
Monsoon	145	0.721	120.086	0.750	114.307	0.747	121.960	0.696	126.124

Parabolic function found to be better fit than other functions from the entire regression analysis with a R<sup>2</sup> of 0.783 and minimum standard error estimate of  $\pm 24.052 \mu\text{atm}$ . The derived  $p\text{CO}_2$  algorithm was used to generate the  $p\text{CO}_2$  image. The  $p\text{CO}_2$  algorithm implies the following equation:

$$p\text{CO}_2 = 1025.6820 - 7.7794 * \text{SST} + 6.0874 * \text{Chl} - 0.5777 * \text{SST}^2 + 19.9015 * \text{Chl}^2$$

Where,  $p\text{CO}_2$  = Partial pressure of carbon dioxide, SST = Sea surface temperature

Chl = Chlorophyll concentration, N = Number of points

### **Satellite data**

To generate remotely sensed  $p\text{CO}_2$  image, satellite derived SST and chlorophyll  $a$  data were required. For remote sensing measurements in the southwest Bay of Bengal, February to May is good period for getting cloud free data, on the other part of the year only rare and sporadic data sets alone available because of the influence of both southwest and northeast monsoons which makes southern Bay of Bengal as more cloud prone area in the northern Indian Ocean region. Hence, MODIS-Aqua derived Level-2a SST and chlorophyll data products for the date 11<sup>th</sup> February 2017 with a spatial resolution of 1km were acquired from the <http://modis.gsfc.nasa.gov>. The data were processed to generate SST and chlorophyll image using ERDAS IMAGINE (ver. 9.2.), SeaDAS (Ver. 7.3.2.) and ENVI (ver.4.7.) software. The datasets were applied to geometric correction to remove the image distortion and bring them to a standard geographic projection (Lat/Lon) with modified Everest Datum.

### **Evaluation criteria**

The evaluation process was made by comparing satellite derived values with the field measurements. Statistical fitting was applied to these data using SigmaPlot (Ver.12.0) statistical software. Mean Normalized Bias (MNB), Standard Error of Estimate (SEE) and Root Mean Square Error (RMSE) were analyzed to test the performance of the algorithms. Mean normalized bias is a measure of the over or underestimation of the true values. Root mean square error provides a good measure of data scatter for normally distributed variables and gives useful information of the accuracy between satellite and *in-situ* data.

## **3. RESULTS AND DISCUSSION**

The oceanic partial pressure of  $\text{CO}_2$  ( $p\text{CO}_2$ ) is highly variable and it is difficult to assess spatial and temporal variability because of the paucity of measurements. In general,  $p\text{CO}_2$  is strongly correlated with sea surface temperature (SST). Even in oceanic regions where physical and biological factors are significant, the  $p\text{CO}_2$  remain be strongly correlated with SST. SST has a dual impact on  $p\text{CO}_2$ . On one hand, the equilibrium of carbonate system in seawater would alter due to the influence of SST in the absence of external exchange. Thereby  $p\text{CO}_2$  will be enhanced as temperature rises<sup>25</sup>. On the other hand, the solubility of carbon dioxide in seawater decreases as temperature increases, which leads to a decrease of  $p\text{CO}_2$ <sup>1</sup>. The chlorophyll is capable of altering the carbonic acid cycle with its primary productivity and respiration. Hence, the three dimensional approach of SST, chlorophyll and  $p\text{CO}_2$  regression fits are attempted to understand the role of SST and chlorophyll on  $p\text{CO}_2$  in the southwest Bay of Bengal coastal waters.

### **Development of $p\text{CO}_2$ algorithm based on in-situ SST and chlorophyll $a$**

The regression analysis between *in-situ* SST, chlorophyll  $a$  and calculated  $p\text{CO}_2$  was

carried out for four different three dimensional functions viz. plane, paraboloid, Gaussian and Lorentzian. The regression equations are given below:

**Entire dataset (N=580)**

$$pCO_2 = 1659.9047 - 46.7099 * SST + 59.7721 * Chl \rightarrow (1) \text{Plane}$$

$$pCO_2 = 3378.7004 - 162.7676 * SST + 46.6872 * Chl + 1.9715 * SST^2 + 1.3970 * Chl^2$$

$\rightarrow (2) \text{Paraboloid}$

$$pCO_2 = 1482.9996 * \exp(-0.5 * ((SST - 21.8135)/(-7.3584))^2 + ((Chl - 15.8418)/10.9075)^2)$$

$\rightarrow (3) \text{Guassian}$

$$pCO_2 = 1314.3895 / ((1 + ((SST - 23.9130)/6.8894)^2) * (1 + ((Chl - 12.4741)/9.9683)^2))$$

$\rightarrow (4) \text{Lorentzian}$

**Postmonsoon (N=165)**

$$pCO_2 = 1447.4029 - 39.6711 * SST + 46.5801 * Chl \rightarrow (5) \text{Plane}$$

$$pCO_2 = 1025.6820 - 7.7794 * SST + 6.0874 * Chl - 0.5777 * SST^2 + 19.9015 * Chl^2$$

$\rightarrow (6) \text{Paraboloid}$

$$pCO_2 = 3315.3998 * \exp(-0.5 * ((SST + 1750771883.6265)/1078697778.5464)^2 + ((Chl - 6.8488)/4.584)^2)$$

$\rightarrow (7) \text{Guassian}$

$$pCO_2 = 522.4279 / ((1 + ((SST + 42.4186)/(-211512.256))^2) * (1 + ((Chl - 2.954)/2.9575)^2))$$

$\rightarrow (8) \text{Lorentzian}$

**Summer (N=120)**

$$pCO_2 = 1776.7438 - 50.6222 * SST + 63.1597 * Chl \rightarrow (9) \text{Plane}$$

$$pCO_2 = 3796.4168 - 174.7775 * SST - 1.17778 * Chl + 1.9237 * SST^2 + 27.3216 * Chl^2$$

$\rightarrow (10) \text{Paraboloid}$

238 *R.Shanthi, D.Poornima, T.Thangaradjou, A.Saravanakumar, S.B.Choudhry*

$$pCO_2 = 502.2731 * \exp(-0.5 * ((SST - 109275.1995) / 197788508.4115)^2 + ((Chl - 2.499) / 1.9359)^2) \\ \rightarrow (11) \text{Guassian}$$

$$pCO_2 = 502.2731 / ((1 + ((SST + 119216.007) / (-60993449.624))^2) * (1 + ((Chl - 2.7029) / 2.3569)^2)) \\ \rightarrow (12) \text{Lorentzian}$$

### **Premonsoon (N=150)**

$$pCO_2 = 2449.5745 - 71.5094 * SST + 16.8118 * Chl \rightarrow (13) \text{Plane}$$

$$pCO_2 = 16901.2522 - 1056.7893 * SST + 18.8756 * Chl + 16.7786 * SST^2 - 0.6697 * Chl^2 \\ \rightarrow (14) \text{Paraboloid}$$

$$pCO_2 = 17301.9896 * \exp(-0.5 * ((SST + 2.0725) / 12.5839)^2 + ((Chl - 39.1642) / 31.2197)^2) \\ \rightarrow (15) \text{Guassian}$$

$$pCO_2 = 2390.7451 / ((1 + ((SST - 21.0947) / 4.0488)^2) * (1 + ((Chl - 12.2996) / 21.0347)^2)) \\ \rightarrow (16) \text{Lorentzian}$$

### **Monsoon (N=145)**

$$pCO_2 = 2838.4296 - 83.5165 * SST + 33.3749 * Chl \rightarrow (17) \text{Plane}$$

$$pCO_2 = -2546.5231 + 302.3587 * SST - 27.6913 * Chl - 6.7814 * SST^2 + 6.7575 * Chl^2 \\ \rightarrow (18) \text{Paraboloid}$$

$$pCO_2 = 1382.6457 * \exp(-0.5 * ((SST - 3999570.0953) / (5335726006.6683))^2 \\ + ((Chl - 1602.4147) / 768.7063)^2) \rightarrow (19) \text{Guassian}$$

$$pCO_2 = 1505.4029 / ((1 + ((SST - 9356374.863) / 286260419.8715)^2) \\ * (1 + ((Chl - 14.6659) / 8.581)^2)) \rightarrow (20) \text{Lorentzian}$$

The entire dataset was regressed at first without considering seasonal variations which represents the significant relationship between *in-situ* variables of entire dataset for plane ( $R^2 = 0.804$ ,  $\text{SEE} = \pm 76.174$ ), paraboloid ( $R^2 = 0.809$ ,  $\text{SEE} = \pm 75.266$ ), Gaussian ( $R^2 = 0.815$ ,  $\text{SEE} = \pm 74.104$ ) and Lorentzian ( $R^2 = 0.811$ ,  $\text{SEE} = \pm 74.811$ ) functions. Though coefficient of determination is found to be significant for all the functions, the standard error of estimate was high. Hence, the regression analysis with seasonal difference was thought off for retrieving  $p\text{CO}_2$  fields, because the seasonal change of SST and chlorophyll *a* have obvious effect on the  $p\text{CO}_2$  algorithm as these input variables were subject to high seasonal differences in this part of the Bay of Bengal.

In the seasonal regression analysis, the  $R^2$  values obtained for different functions and seasons are summarized in table 1. Among the four functions, the parabolic function found to be better fit for the entire and seasonal datasets. The parabolic function provides the highest determination coefficient ( $R^2 = 0.809$ ,  $\text{SEE} = \pm 75.266$ ) for entire dataset and the lowest  $R^2$  values of 0.700 and 0.749 with the SEE of  $\pm 42.370$  and  $\pm 46.224$  obtained for summer and premonsoon seasons respectively. During premonsoon, the highest chlorophyll *a* concentrations associated with moderate SST, indicating that both SST and chlorophyll have a mutual control on  $p\text{CO}_2$ . During summer the biological productivity is low due to the high SST and diminished nutrients, under these conditions the  $p\text{CO}_2$  concentration is largely influenced by SST rather than chlorophyll *a*. The low chlorophyll *a* concentrations and high SST suggesting that SST might have a major control on  $p\text{CO}_2$  as opined by Chierici et al.<sup>26</sup>. Moreover, the stratified nature of the water column observed during postmonsoon leads to the lowest biological activities due to the absence of nutrients at the surface waters<sup>27</sup> hence, the SST has a predominant control over the  $p\text{CO}_2$  distribution in the Bay of Bengal. Finding a  $p\text{CO}_2$ -chlorophyll and  $p\text{CO}_2$ -SST fit does not mean that only biological or physical mechanisms are at work, but rather a complexity of interactions determines the small scale variations in  $p\text{CO}_2$ , hence, biological contribution must be included in  $p\text{CO}_2$  model as the biological activity tends to be higher in warm water<sup>28</sup>.

Though, the entire dataset exhibit the better fit than other seasonal datasets, the regression analysis of postmonsoon dataset results the minimum SEE  $\pm 24.052$  with significant  $R^2$  (0.783). Hence, the postmonsoon parabolic equation (6) is further utilized for the generation of remotely sensed  $p\text{CO}_2$  maps.

### Validation of MODIS-Aqua derived SST

MODIS derived SST data (Fig.2a) was validated with *in-situ* SST to evaluate the performance of MODIS-Aqua and exhibited the good agreement with significant correlation co-efficient ( $R^2$ ) of 0.887 with SEE of  $\pm 0.179$ , MNB of -0.104 and RMSE of 3.168°C (Fig.2b). The data points fall outside of the 95% confidence band suggest that the satellite derived values were higher or lower than they should be in natural waters. However, the comparison plot of *in-situ* SST with MODIS derived SST showed that the 100% of the *in-situ* data were underestimated by the MODIS-SST

(Fig.2c). However, the regression fit found significant with correlation of  $R^2 = 0.887$  hence, MODIS derived SST data was utilized to generate remotely sensed  $p\text{CO}_2$  map.

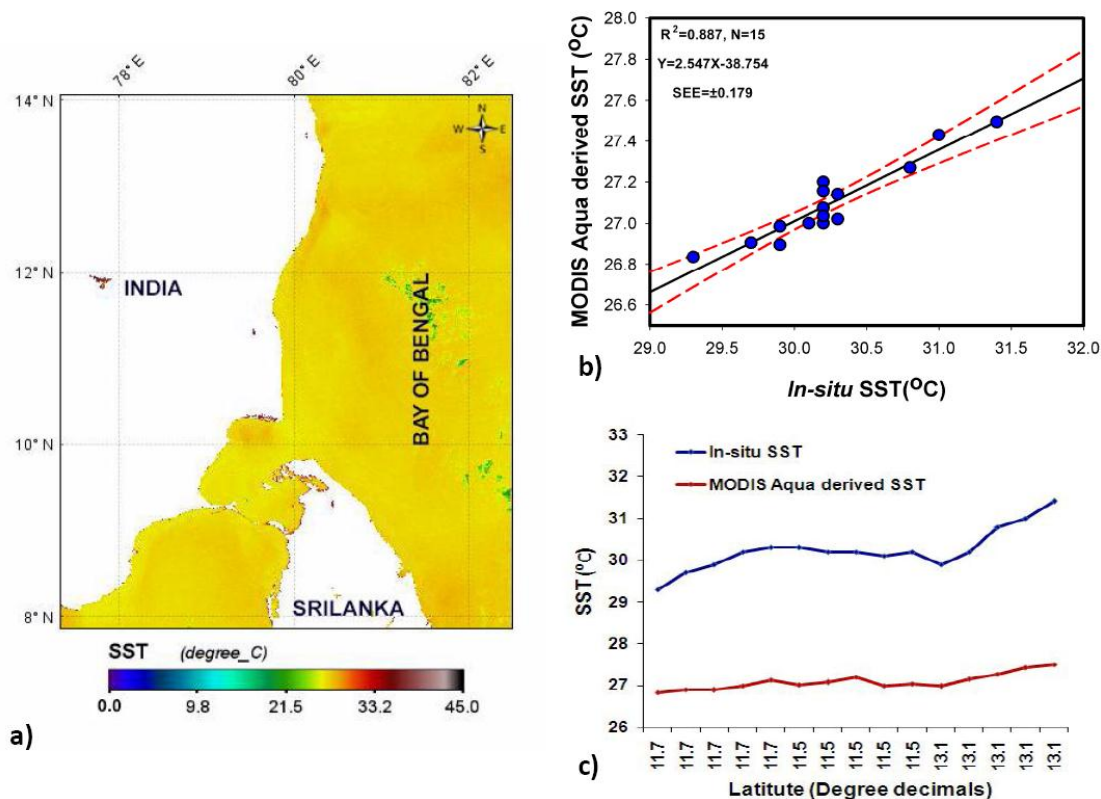


**Fig. 2.** MODIS-Aqua derived SST image of 11<sup>th</sup> February 2017 (a) and regression (b) and comparison (c) plots of *in-situ* SST Vs MODIS-Aqua derived SST

Evaluation of MODIS-SST with *in-situ* SST shows the negative bias (MNB =  $-0.104$ ) with RMSE of  $\pm 3.168^\circ\text{C}$  which is greater than the error ( $\pm 0.38^\circ\text{C}$ ) observed by Gentemann (2014) and could be attributed to possible errors in cloud removal, aerosol contaminated retrievals, or sampling. Moreover, SST measured using infrared radiometers will estimate with high resolution only under cloud free conditions and it has been clearly evident from the regression results ( $R^2=0.887$  and  $SEE \pm 0.179^\circ\text{C}$ ). The statistical results obtained in this study are comparable to MODIS SST validation with *in-situ* measurements along the western Pacific coasts<sup>29</sup> with a bias of  $-0.32^\circ\text{C}$ ; western North Pacific<sup>30</sup> with a bias of  $-0.06^\circ\text{C}$  and RMSE of  $\pm 0.81^\circ\text{C}$ , Taiwan coast<sup>31</sup> with a bias of  $0.42^\circ\text{C}$  and RMSE of  $\pm 0.86^\circ\text{C}$ , San Matías Gulf of Argentina<sup>32</sup> with a  $R^2$  of 0.89 and Bay of Bengal<sup>33</sup> with a bias of  $1.80^\circ\text{C}$  and reported the overestimation of the satellite product.

### Validation of MODIS-Aqua derived chlorophyll

The relationship between the *in-situ* and MODIS chlorophyll exhibited the fairly good agreement with correlation co-efficient ( $R^2$ ) of 0.731, SEE of  $\pm 0.207\mu\text{g l}^{-1}$  and RMSE

of  $0.246\mu\text{gl}^{-1}$  (Fig. 3a and 3b). MODIS derived chlorophyll shows the 33% underestimation and 67% overestimation of *in-situ* chlorophyll (Fig.3c) which is confirmed by the large positive bias of 0.184. Present algorithm (chlor\_a\_2) of MODIS overestimates the chlorophyll concentration at low concentrations around  $<1.0\mu\text{gl}^{-1}$  of chlorophyll along the coastal waters. This study agrees with the previous studies of Xiu et al.<sup>35</sup>, Montres et al.<sup>36</sup> and Poornima et al.<sup>27</sup> using MODIS data.

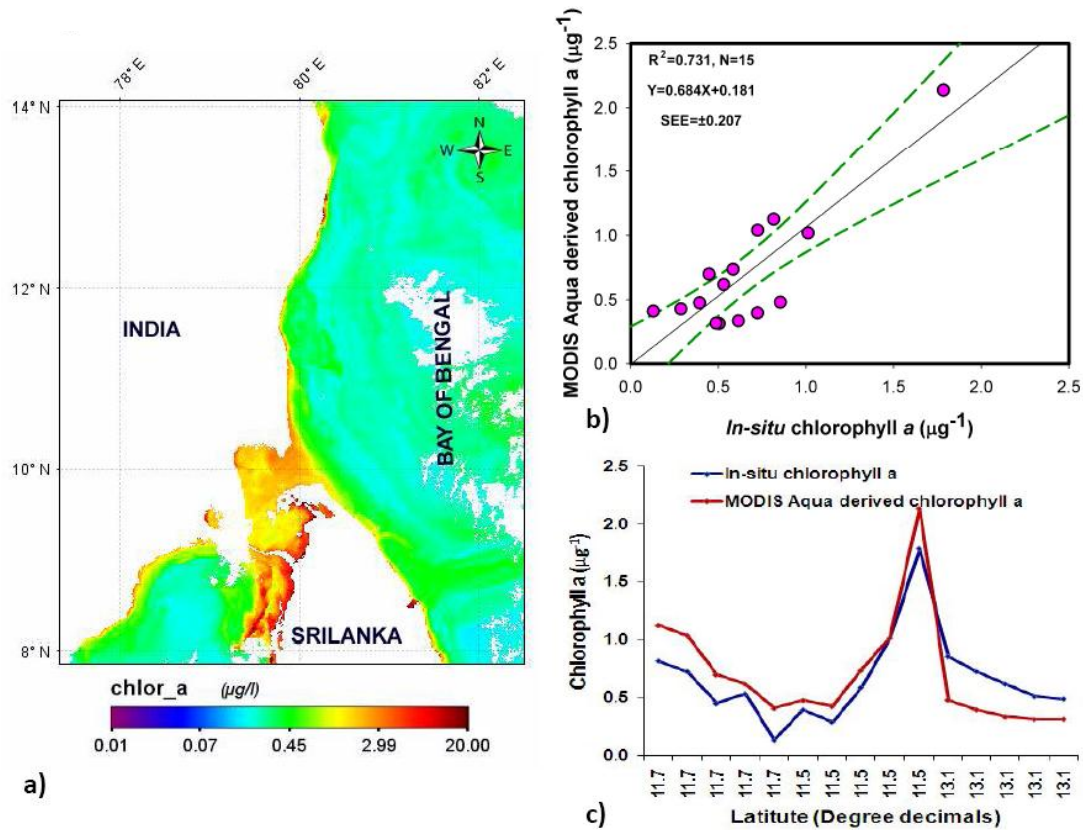


**Fig. 3.** MODIS-Aqua derived chlorophyll-*a* image of 11<sup>th</sup> February 2017 (a) and regression (b) and comparison (c) plots of *in-situ* chlorophyll *a* Vs MODIS-Aqua derived chlorophyll *a*

Possibly, the overestimation of chlorophyll could be due to the interference of suspended sediment and CDOM in the water leaving radiances. Besides this, other possible sources of errors are also identified and are bottom effects<sup>37</sup>, the mixtures of organic and inorganic suspensions<sup>38</sup>, absorption due to CDOM<sup>39</sup> and turbulent effect of wind agitation. MODIS will probably continue to be executed indiscriminately for all waters of the world's oceans with standard algorithms designed primarily for case 1 waters and at present the NASA adopted OC3M algorithm for the global MODIS processing. Moreover, global algorithms for satellite remote sensing do not always provide reasonable retrievals in all areas of the ocean, because an empirical algorithm is only as good as the data for specific environment or bio-optical provinces where the algorithm is to be applied<sup>40</sup>.

### Validation of remotely sensed $p\text{CO}_2$

The two parameter (SST and Chlorophyll  $a$ ) parabolic algorithm of  $p\text{CO}_2$  showed better agreement with *in-situ*  $p\text{CO}_2$  measurements with a  $R^2$  of 0.755 and SEE of  $\pm 23.609$  (Fig. 4a - c). This suggests that the effects of biological activities on the spatial and temporal changes in  $p\text{CO}_2$  of the southwest Bay of Bengal cannot be ignored. Hence, algorithm based on SST and chlorophyll  $a$  is better fit for the region. However, the RMSE ( $\pm 27.156 \mu\text{atm}$ ) and MNB (0.040) of SST and chlorophyll based algorithm is appreciably higher than RMSE ( $\pm 14$  and  $\pm 17 \mu\text{atm}$ ) reported by Ono et al.<sup>16</sup> in large areas of subtropical and sub-polar North Pacific Ocean respectively. Similarly, Zhu et al.<sup>9</sup> recorded the improvement of  $p\text{CO}_2$  algorithm by the inclusion of chlorophyll  $a$  with RMSE of  $\pm 4.5 \mu\text{atm}$ . On the other hand, Olsen et al.<sup>41</sup> obtained an error of  $\pm 9.5 \mu\text{atm}$  from measurements gathered in the Caribbean Sea using different algorithm based on linear relationship between SST and  $p\text{CO}_2$  including geographical location. Comparitively higher RMSE in the present study is due to the inbound error in SST and chlorophyll images with higher percentage of cloud cover. The error in SST and chlorophyll estimation reported for the MODIS data would definitely cascade with the  $p\text{CO}_2$  measurements.

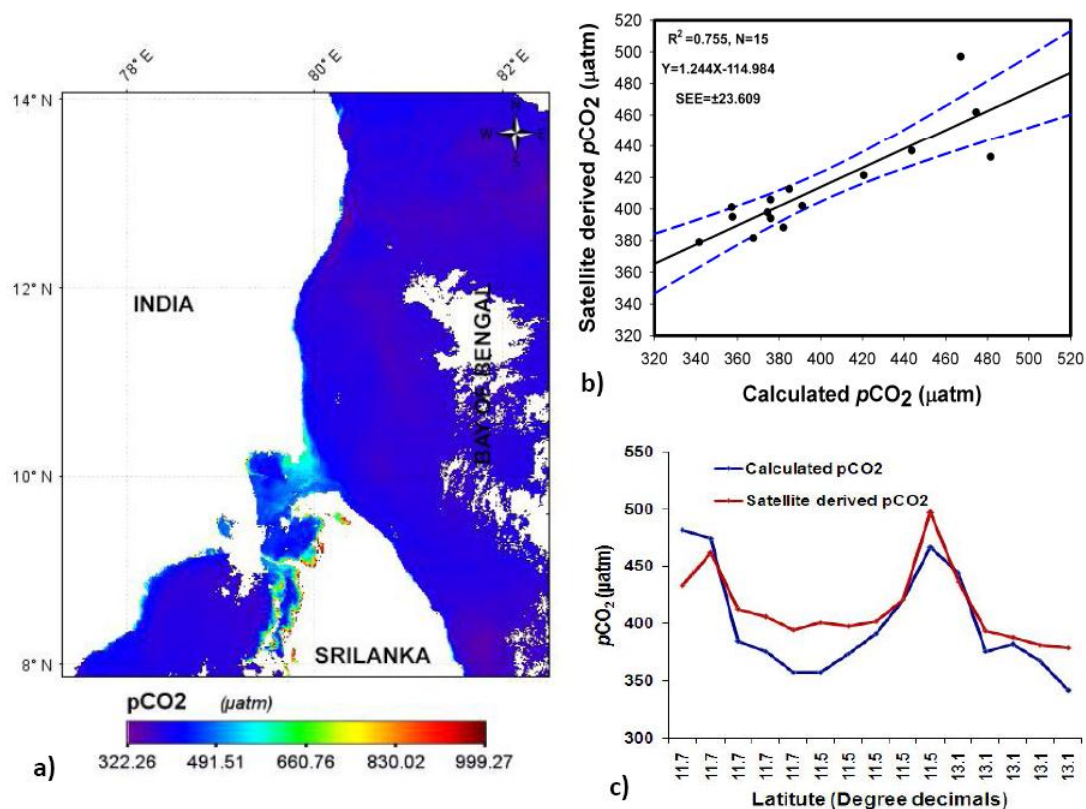


**Fig. 4.** SST and chlorophyll  $a$  based satellite derived  $p\text{CO}_2$  image of 11<sup>th</sup> February 2017 (a) and regression (b) and comparison (c) plots of calculated  $p\text{CO}_2$  Vs satellite derived  $p\text{CO}_2$  using MODIS-Aqua derived SST and chlorophyll

Lohrenz and Cai<sup>19</sup> described  $p\text{CO}_2$  algorithm using temperature, salinity derived from chromophoric dissolved organic matter (CDOM) and chlorophyll with a  $R^2 = 0.838$  of satellite derived  $p\text{CO}_2$  with shipboard measurements. The  $p\text{CO}_2$  algorithms developed based on *in-situ* SST, chlorophyll and climatological salinity exhibited the RMSE of 17-20 $\mu\text{atm}$  with *in-situ*  $p\text{CO}_2$  data<sup>17</sup>. Padin et al.<sup>18</sup> applied the empirical algorithm described by Ono et al.<sup>16</sup> for predicting  $f\text{CO}_2$  measurements in the Bay of Biscay from remotely sensed SST and chlorophyll  $a$  with a residual error of  $0.1 \pm 7.5 \mu\text{atm}$ . Similarly, Chierici et al.<sup>26</sup> predicted  $f\text{CO}_2$  with a standard error of  $\pm 13 \mu\text{atm}$  using SST and chlorophyll  $a$  based algorithm, the SST, chlorophyll  $a$  and mixed layer depth (MLD) based prediction of  $f\text{CO}_2$ <sup>42</sup> and matched with *in-situ* data (RMSE =  $\pm 11 \mu\text{atm}$ ) and Zui et al.<sup>20</sup> reported two parameter algorithm and found that the two parameter (SST and chlorophyll) algorithm worked better (RMSE =  $\pm 15.82 \mu\text{atm}$ ) with the relative error of less than 4.25%. Recently, Qin et al.<sup>1</sup> modified the Ono's equation by removing the second order variable of chlorophyll  $a$  to obtain a good retrieval of  $p\text{CO}_2$  in the Yellow Sea and got RMSE of  $\pm 16.68 \mu\text{atm}$ .

The seasonal regression analysis showed the significant seasonal variability in the relationship of  $p\text{CO}_2$  with SST and chlorophyll  $a$ . The  $p\text{CO}_2$  and SST had a strong inverse relationship in all the seasons suggesting that increased SST reduce the dissolution of  $\text{CO}_2$  in seawater, thereby decreases the  $p\text{CO}_2$  in seawater. The error in the satellite derived  $p\text{CO}_2$  map is mainly because of the inbound errors in MODIS derived SST and chlorophyll data products. Hence, improvement in sensor technology and retrieval algorithm would definitely improve the retrieval of input parameters (SST and Chlorophyll  $a$ ) which in turn useful in estimating  $p\text{CO}_2$  precisely. This would enable us to understand biogeochemical processes behind the variability of  $\text{CO}_2$  in the surface waters of the southwest Bay of Bengal

#### 4. CONCLUSION

The significant agreement between the SST and chlorophyll  $a$  based algorithm derived  $p\text{CO}_2$  and calculated  $p\text{CO}_2$  suggesting that the remote sensing technique is applicable to air-sea  $\text{CO}_2$  flux observations in the southwest Bay of Bengal. The collection of more *in-situ* data covering various temporal and spatial scales is necessary in order to improve the algorithm. It should be noted that this work is limited to the preliminary results for the southwest Bay of Bengal in the postmonsoon season. Whether this applicable to other regions of the Bay of Bengal and for other seasons requires further investigation.

#### ACKNOWLEDGEMENTS

Authors are thankful to the Director and Dean and the authorities of Annamalai University for their support and encouragement. The authors also thank the National Remote Sensing Centre, ISRO, Government of India, Hyderabad for financial assistance through NCP-Coastal Carbon Dynamics Study. The contents and views reported in the manuscript are of the individual authors and not expressing the position or view of the organizations they present.

**REFERENCES**

- [1] **Qin, B. Y., Tao, Z., Li, Z. W. and Yang, X. F.**, 2014, "Seasonal changes and controlling factors of sea surface  $p\text{CO}_2$  in the Yellow Sea," IOP conference series: Earth Environ. Sci., 17, 012025.
- [2] **Takahashi T.**, 1989, "Could the oceans be the store house for the emitting gas?," *Oceanus.*, 32, 22-29.
- [3] **Kumar, M. D., Rajendran, A., Somasundar, K., Ittekkot, V., and Desai, B. N.**, 1992, "Processes controlling carbon components in the Arabian Sea," *Oceanogr. Indian Ocean*, pp. 313-325.
- [4] **George, M. D., Dileep Kumar, M., Naqvi, S. W. A., Banerjee, S., Narekar, P. V., de Sousa, S. N., and Jayakumar, D. A.**, 1994, "Study of the carbon dioxide system in the northern Indian Ocean during premonsoon," *Mar. Chem.*, 47, 243-254.
- [5] **Sarma, V. V. S. S., Dileep Kumar, M., and George, M. D.**, 1998, "The central and Eastern Arabian Sea as a perennial source of atmospheric carbon dioxide," *Tellus-B*, 50, 179-184.
- [6] **Kumar, M. D., Naqvi, S. W. A., George, M. D., and Jayakumar, D. A.**, 1996, "A sink for atmospheric carbon dioxide in the northeast Indian Ocean," *J. Geophys. Res.*, 101, 18121-18125.
- [7] **Mintrop, L., Kortzinger, A., and Duinker, J. C.**, 1999, "The carbon dioxide system in the northwestern Indian Ocean during south-west monsoon," *Mar. Chem.*, 64, 315 – 336.
- [8] **Stephens, M. P., Samuels, G., Olson, D. B., Fine, R. A., and Takahashi, T.**, 1995, "Sea-air flux of  $\text{CO}_2$  in the North Pacific using shipboard and satellite data," *J. Geophys. Res.*, 100, 13571-13583.
- [9] **Zhu, Y., Shag, S., Zhai, W., and Dai, M.**, 2009, "Satellite-derived surface water  $p\text{CO}_2$  and air- sea  $\text{CO}_2$  fluxes in the northern South China Sea in Summer," *Prog. Nat. Sci.*, 19, 775-779.
- [10] **Conkright, M. E., Levitus, S., Boyer, T. P., Bartolacci, D., and Luther, M.**, 1994, "Atlas of the Northern Indian Ocean," Univ. South Fla., St. Petersburg, 157 pp.
- [11] **Murnane, R. J., Sarmiento, J. L. and LeQue´re´, C.**, 1999, "The spatial distribution of air-sea fluxes and the inter hemispheric transport of carbon by the oceans," *Global Biogeochem. Cyc.*, 13, pp. 287-305.
- [12] **Feely, R. A., Sabine, C. L., Takahashi, T., and Wanninkhof, R.**, 2001, "Uptake and storage of carbon dioxide in the Ocean: The Global  $\text{CO}_2$  survey," *Oceanogr.*, 14(4), pp. 18-32.
- [13] **Goyet, C., Millero, F. J., O'Sullivan, D. W., Eisheid, G., McCue, S. J., and Bellerby, R. G. J.**, 1998, "Temporal variations of  $p\text{CO}_2$  in surface seawater of

- the Arabian Sea in 1995,” *Deep Sea Res.*, 145, pp. 609-623.
- [14] **Nelson, N.B., Bates, N.R., Siegel, D.A., and Michaels, A.F.**, 2001, “Spatial variability of the  $\text{CO}_2$  sink in the Sargasso Sea,” *Deep-Sea Res.* –II., 48, pp. 1801–1821.
- [15] **Cosca, C. E., Feely, R. A., Boutin, J., Etcheto, J., McPhaden, M. J., Chavez, F. P., and Strutton, P. G.**, 2003, “Seasonal and inter-annual  $\text{CO}_2$  fluxes for the central and eastern equatorial Pacific Ocean as determined from  $f\text{CO}_2$ -SST relationships,” *J. Geophys. Res.*, 108(C8), 3278 doi:10.1029/2000JC000677.
- [16] **Ono, T., Saino, T., Kurita, N., and Sasaki, K.**, 2004, “Basin-scale extrapolation of shipboard  $p\text{CO}_2$  data by using satellite SST and Chl a,” *Int. J. Rem. Sens.*, 25(19), pp. 803-815.
- [17] **Sarma, V. V. S. S., Saino, T., Sasaoka, K., Nojiri, Y., Ono, T., Ishii, M., Inoue, H.Y., and Matsumoto, K.**, 2006, “Basin-scale  $p\text{CO}_2$  distribution using satellite sea surface temperature, Chl a, and climatological salinity in the North Pacific in spring and summer,” *Global Biogeochem. Cyc.*, 20, GB3005.
- [18] **Padin, X.A., Navarro, G., Gilcoto, M., Rios, A.F., and Pérez, F.F.**, 2009, “Estimation of air-sea  $\text{CO}_2$  fluxes in the Bay of Biscay based on empirical relationships and remotely sensed observations,” *J. Mar. Syst.*, 75, pp. 280-289.
- [19] **Lohrenz, S. E., and Cai, W.J.**, 2006, “Satellite ocean color assessment of air-sea fluxes of  $\text{CO}_2$  in a river-dominated coastal margin,” *Geophys. Res. Lett.*, 33, L01601.
- [20] **Zui, T. A. O., Bangyong, Q. I. N., Ziwei, L. I., and Xiaofeng, Y.**, 2012, “Satellite observations of the partial pressure of carbon dioxide in the surface water of the Huanghai Sea and the Bohai Sea,” *Acta Oceanol. Sin.*, 31(3), pp. 67-73.
- [21] **SATCORE**, 2009, “Sampling strategy In: Technical report,” Lotliker, A. A., Vijayan, A. K., and Kumar, T. S. (eds.), INCOIS, Hyderabad, pp. 1-33.
- [22] **Gran, G.**, 1952, “Determination of the equivalence point in potentiometric titrations, Part II,” *Analyst.*, 77, 661-671.
- [23] **Robbins, L. L., Hansen, M. E., Kleypas, J. A., and Meylan, S. C.**, 2010, “ $\text{CO}_2$ calc: A user- friendly seawater carbon calculator for windows, Mac OS X, and iOS (iPhone). Florida Shelf Ecosystems Response to Climate Change Project,” Open-File Report 2010-1280, U.S. Department of the Interior, U.S. Geological Survey.
- [24] **Lueker, T. J., Dickson, A. G., and Keeling, C. D.**, 2000, “Ocean  $p\text{CO}_2$  calculated from dissolved inorganic carbon, alkalinity, and equations for  $K_1$  and  $K_2$ —Validation based on laboratory measurements of  $\text{CO}_2$  in gas and seawater at equilibrium,” *Mar. Chem.*, 70, pp. 105-119.
- [25] **Copin-Montegut, C.**, 1988, “A new formula for the effect of temperature on the partial pressure of carbon dioxide in sea water,” *Mar. Chem.*, 25, pp. 29-37.

- [26] **Chierici, M., Signorini, S. R., Mattsdotter-björk, M., Fransson, A., and Olsen, A.**, 2012, "Surface water  $f\text{CO}_2$  algorithms for the high-latitude Pacific sector of the Southern Ocean Pacific sector," *Rem. Sens. Environ.*, 119, pp. 184-196.
- [27] **Poornima, D., Shanthi, R., Raja, S., VijayabaskaraSethubathi, G., Thangaradjou, T., Balasubramanian, T., Babu, K.N., and Shukla, A.K.**, 2013, "Understanding the Spatial Variability of Chlorophyll a and Total Suspended Matter distribution along the Southwest Bay of Bengal Using In-Situ and OCM-2 & MODIS-Aqua Measurements," *J. Indian Soc. Rem. Sens.*, 2524-012-0233-4.
- [28] **Rangama, Y., Boutin, J., Etcheto, J., Merlivat, L., Takahashi, T., Delille, D., et al.**, 2005, "Variability of the net air-sea  $\text{CO}_2$  flux inferred from shipboard and satellite measurements in the Southern Ocean south of Tasmania and New Zealand," *J. Geophys. Res.*, 110, C09005.
- [29] **Gentemann, C. L.**, 2014, "Three way validation of MODIS and AMSR-E sea surface temperatures," *J. Geophys. Res. – Oceans.*, 119, 2583-2598.
- [30] **Barton, I., and Pearce, A.**, 2006, "Validation of GLI and Other Satellite-Derived Sea Surface Temperatures Using Data from the Rottneest Island Ferry, Western Australia," *J. Oceanogr.*, 62, 303-310.
- [31] **Hosoda, K., Murakami, H., Sakaida, F., and Kawamura, H.**, 2007, "Algorithm and Validation of Sea Surface Temperature Observation Using MODIS Sensors aboard Terra and Aqua in the Western North Pacific," *J. Oceanogr.*, 63, pp. 267-280.
- [32] **Lee, T., Hakkinen, S., Kelly, K., Qiu, B., Bonekamp, H., and Lindstrom, E.J.**, 2010, "Satellite observations of ocean circulation changes with climate variability," *Oceanogr.*, 23(4), pp. 70-81.
- [33] **Williams, G. N., Dogliotti, A. I., Zaidman, P., Solis, M., Narvarte, M. A., Gonzalez, R. C., Estevez, J. L., Gagliardini, D. A.**, 2013, "Assessment of Remotely-Sensed Sea Surface Temperature and Chlorophyll-a Concentration in San Matías Gulf (Patagonia, Argentina)," *Cont. Shelf Res.* 52, pp. 159-171.
- [34] **34. Narayanan, M., Vasan, D. T., Bharadwaj, A. K., Thanabalan, P., and Dhileeban, N.**, 2013, "Comparison and validation of sea surface temperature (SST) using MODIS and AVHRR sensor data," *Geosciences*, 2(3), pp. 1-7.
- [35] **Xiu, P., Liu, Y. G., Rong, Z., Zong, H., Li, G., Xing, X., and Cheng, Y.**, 2007, "Comparison of chlorophyll algorithms in the Bohai Sea of China," *Ocean Sci J.*, 42(4), 199-209.
- [36] **Montres, H. M. A., Vernet, M., Smith, R., and Carder, K.L.**, 2008, "Phytoplankton size structure on the western shelf off the Antarctic Peninsula: A remote sensing approach," *Int. J. Rem. Sens.*, 29(3&4), pp. 801-829.
- [37] **Rundquist, D. C., Schalles, J. F., and Peake, J. S.**, 1995, "The response of

- volume reflectance to manipulated algal concentrations above bright and dark bottoms at various depths in an experimental pool,” *Geocarto Int.*, 10, pp. 5-14.
- [38] **Dekker, A. G.**, 1993, “Detection of optical water quality parameters for eutrophic waters by high resolution remote sensing,” Ph.D. Thesis, Free University, Amsterdam, pp. 1-240.
- [39] **Liew, S. C., Chia, A. S., and Kwoh, L. K.**, 2001, “Evaluating the validity of SeaWiFS chlorophyll algorithm for coastal water; In: Proceeding of ACRS 2001 - 22<sup>nd</sup> Asian Conference on Remote Sensing 5–9 November 2001,” Singapore 2, pp. 939-943.
- [40] **IOCCG**, 2006, “Remote Sensing of Inherent Optical Properties: Fundamentals, Tests of Algorithms, and Applications,” **Lee, Z. P.** (ed.) Reports of the International Ocean-Colour Coordinating Group, No. 5, IOCCG, Dartmouth, Canada.
- [41] **Olsen, A., Trinanes, J. A., and Wanninkhof, R.**, 2004, “Sea-air flux of  $\text{CO}_2$  in the Caribbean Sea estimated using *in situ* and remote sensing data,” *Rem. Sens. Environ.*, 89, pp. 309-325.
- [42] **Chierici, M., Signorini, S. R., Mattsdotter-björk, M., Fransson, A., and Olsen, A.**, 2012, “Surface water  $f\text{CO}_2$  algorithms for the high-latitude Pacific sector of the Southern Ocean Pacific sector,” *Rem. Sens. Environ.*, 119, pp.184-196.

